Ground-state spin of ^{59}Mn

M. Oinonen, V. Fedoseyev, V. Mishin, J. Huikari, A. Jokinen, A. Nieminen, K. Perajarvi, J. Aysto, A. Knipper, G. Walter, et al.

Eur. Phys. J. AP **10**, 123–130 (2000)

THE EUROPEAN PHYSICAL JOURNAL APPLIED PHYSICS

Modeling and experimental characterization of saturation effect of an induction machine

T. Kasmieh[1,a], Y. Lefevre[2], and J.C. Hapiot[2]

[1] LAE, HIAST[b], BP 60318 Damascus, Syria
[2] LEEI, INPT[c], BP 7122, 31071 Toulouse Cedex 7, France

Received: 22 June 1999 / Revised and Accepted: 26 January 2000

Abstract. This paper presents a new experimental measurement method of the electrical parameters, shown from the stator, of a squirrel cage induction machine in accordance with its magnetic saturation level. It develops a new two-phase saturated model of the induction machine which uses these measured electrical parameters. This new measurement method has a very big advantage in the industrial domain. It avoids the use of a finite elements calculation program which takes much more time to calculate the electrical parameters. The experimental measurement method is applied on a 4 KW squirrel cage induction machine. A comparison between the real dynamic response of this machine, and the dynamic response of the new two-phase saturated model shows that the obtained results are very encouraging.

PACS. 07.05.Tp Computer modeling and simulation

1 Introduction

In modern induction machines design, there is a trend towards increasing the flux densities to obtain higher value of the motor torque at the nominal behavior. Some times, industrial applications demand the motor to operate at a point which is different from the nominal one, to reach a high speed for example. This can cause a bad performance of the dynamic response of the machine if the variation of its electrical parameters is not taken into account by the model.

Many studies concerning the modeling of the induction machine were published to introduce the variation of cyclic inductances with the variation of the saturation level in the air-gap. Most of these studies use a finite elements calculation program [1,5,10]. Other studies tried to find special models based on vector control law [2–4]. Therefore, these models are not general and related to the type of the studied vector control law.

In our recent paper [5], we presented a physical study of the saturation effect in the air gape, and we developed a two-phase saturated model of the induction machine.

In fact, this model was interesting because of its small time of calculation of the dynamic response of the machine. Nevertheless, to be able to deal with it, we were obliged to pass by a finite elements calculation program to calculate all cyclic inductances of the machine which are used by this two-phase saturated model.

In this paper we are going to determine the electrical parameters of the two-phase saturated model that we can see from the stator. Then, we will present a new experimental measurement method of these parameters in accordance with the magnetic state of the machine. The aim of this study is to find another two-phase saturated model that uses these electrical parameters, and avoids the pass by a finite elements calculation program.

2 Revision

To make the approaches in this paper clearer, we will revise in this section the essential points of the establishment of the two-phase saturated model [5,6].

In fact, this model was validated using a finite elements calculation program. This program considers the induction machine as a multiphase electromagnetic system of 3 phases in the stator end m phases in the rotor [7–9]. Since the stator flux space vector and the rotor flux space vector rotate at the same velocity, which is the stator pulsation ω_S, the multiphase model considers that the number of poles in the rotor is equal to the number of poles in the stator. Therefore, the number of rotor phases is equal to $m = q/2p$, where q is the number of rotor bars and p is the number of pole pairs.

The establishment of the two-phase saturated model was done by applying the 3 to 2 phases *Park* transformation in the stator, and the m to 2 phases *Park* transformation in the rotor. The electromagnetic system obtained using these transformations is shown in Figure 1.

[a] e-mail: t_kasmieh@hotmail.com
[b] Higher Institute of Applied Sciences and Technology
[c] Institut National Polytechnique de Toulouse

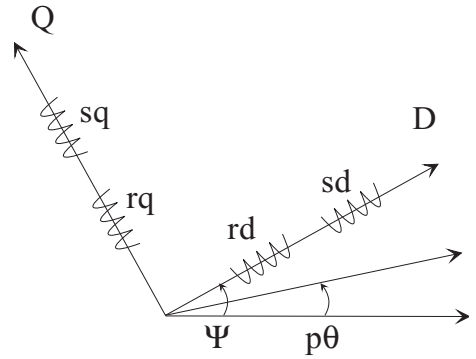

Fig. 1. Two-phase electromagnetic system of the induction machine.

This electromagnetic system can be described by the following general flux-currents relationships:

$$\begin{aligned} \Phi_{sx} &= L_{sx} i_{sx} + M_{srx} i_{rx} \\ \Phi_{rx} &= L_{rx} i_{rx} + M_{rsx} i_{sx} \end{aligned} \tag{1}$$

where x is put for d or q, and the cyclic inductances are functions of the currents (i_{sd}, i_{sq}, i_{rd}, i_{rq}).

The curves of cyclic inductances can be obtained by injecting only one current: $L_{sx} = \Phi_{sx}/i_{sx}$, $L_{rx} = \Phi_{rx}/i_{rx}$, $M_{srx} = \Phi_{sx}/i_{rx}$ and $M_{rsx} = \Phi_{rx}/i_{sx}$.

In paper [5], we demonstrated that the magnetic state of the induction machine depends on the modulus of the magnetizing current vector $|\underline{I_m}| = \sqrt{(i_{sd} + \alpha i_{rd}^{\alpha})^2 + (i_{sq} + \alpha i_{rq}^{\alpha})^2}$, where α is the reference factor. Its expression is given in [7] and it does not depend on the magnetic state of the machine in the contrary of the factor L_s/M which includes the leakage inductance in the numerator that varies with the magnetic state.

The established saturated model can be described by the following electromechanical equations:

– electrical equations:

$$\begin{aligned} \underline{V_s} &= R_s \underline{I_s} + \frac{\mathrm{d}\underline{\Phi_s}}{\mathrm{d}t} + j\frac{\mathrm{d}\Psi}{\mathrm{d}t}\underline{\Phi_s} \\ \underline{0} &= R_r^{\alpha} \underline{I_r^{\alpha}} + \frac{\mathrm{d}\underline{\Phi_r^{\alpha}}}{\mathrm{d}t} + j\frac{\mathrm{d}(\Psi - p\theta)}{\mathrm{d}t}\underline{\Phi_r^{\alpha}} \end{aligned} \tag{2}$$

– flux-current relationships:

$$\begin{aligned} \underline{\Phi_s} &= L_s\left(|\underline{I_m}|\right)\underline{I_s} + M^{\alpha}\left(|\underline{I_m}|\right)\underline{I_r^{\alpha}} \\ \underline{\Phi_r^{\alpha}} &= L_r^{\alpha}\left(|\underline{I_m}|\right)\underline{I_r^{\alpha}} + M^{\alpha}\left(|\underline{I_m}|\right)\underline{I_s} \end{aligned} \tag{3}$$

– mechanical equation:

$$j\frac{\mathrm{d}\Omega}{\mathrm{d}t} = C_{em} - f\Omega - C_r. \tag{4}$$

The index α is adopted for all rotor electrical parameters to show that this model is established for a reference factor α.

Because of the fact that leakage inductances are included in L_s and L_r, this model was called the two-phase saturated model of separated leakage inductances.

From equation (3) we can see that the saturation cross effect is introduced in the cyclic inductances evolutions. For example, the stator flux of the D axis does not vary only with i_{sd} and i_{rd}, but also with i_{sq} and i_{rq} because L_s and M vary with $|\underline{I_m}|$.

3 Electrical parameters shown from the stator

In this section we are going to find the electrical parameters that can experimentally measured from the stator at several saturation levels.

First of all, from the saturated model described before, we will find an equivalent saturated model with a unity reference factor, $\alpha = 1$. This can easily be done by introducing the following new parameters in the electrical equations and in the flux-currents relationships: $\underline{\Phi_r} = \underline{\Phi_r^{\alpha}}/\alpha$, $\underline{I_r} = \alpha \underline{I_r^{\alpha}}$, $M = M^{\alpha}/\alpha$, $L_r = L_r^{\alpha}/\alpha^2$ and $R_r = R_r^{\alpha}/\alpha^2$, so we obtain the equivalent model described by the following electromechanical equations:

– electrical equations:

$$\begin{aligned} \underline{V_s} &= R_s \underline{I_s} + \frac{\mathrm{d}\underline{\Phi_s}}{\mathrm{d}t} + j\frac{\mathrm{d}\Psi}{\mathrm{d}t}\underline{\Phi_s} \\ \underline{0} &= R_r \underline{I_r} + \frac{\mathrm{d}\underline{\Phi_r}}{\mathrm{d}t} + j\frac{\mathrm{d}(\Psi - p\theta)}{\mathrm{d}t}\underline{\Phi_r} \end{aligned} \tag{5}$$

– flux-current relationships:

$$\begin{aligned} \underline{\Phi_s} &= L_s\left(|\underline{I_m}|\right)\underline{I_s} + M\left(|\underline{I_m}|\right)\underline{I_r} \\ \underline{\Phi_r} &= L_r\left(|\underline{I_m}|\right)\underline{I_r} + M\left(|\underline{I_m}|\right)\underline{I_s} \end{aligned} \tag{6}$$

– mechanical equation:

$$j\frac{\mathrm{d}\Omega}{\mathrm{d}t} = C_{em} - f\Omega - C_r \tag{7}$$

where $|\underline{I_m}| = \sqrt{(i_{sd} + i_{rd})^2 + (i_{sq} + i_{rq})^2}$ is the modulus of the magnetising current vector.

Figure 2 shows the electrical circuit of this equivalent model.

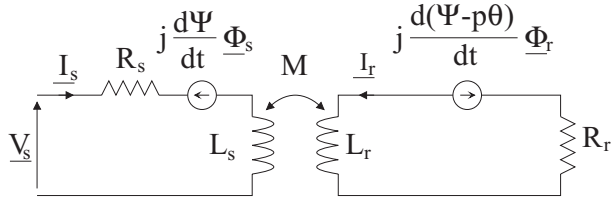

Fig. 2. Equivalent saturated model with a unity reference factor.

For a certain saturation level s, the cyclic inductances do not vary. So, If we apply the 2 to 3 inverse *Park* transformation for $\Psi = 0$ in the stator, and for $\Psi = p\theta$ in the

rotor, we obtain the following electrical equations of each phase:

$$[V_\mathrm{s}]_3 = R_\mathrm{s}[I_\mathrm{s}]_3 + L_\mathrm{s}^s \frac{\mathrm{d}[I_\mathrm{s}]_3}{\mathrm{d}t} + M^s \frac{\mathrm{d}[I_\mathrm{r}]_3}{\mathrm{d}t}$$
$$[0]_3 = R_\mathrm{r}[I_\mathrm{r}]_3 + M^s \frac{\mathrm{d}[I_\mathrm{s}]_3}{\mathrm{d}t} + L_\mathrm{r}^s \frac{\mathrm{d}[I_\mathrm{r}]_3}{\mathrm{d}t}$$

where $[X]_3^t = [x_a,\, x_b,\, x_c]$.

For the a stator phase and the a rotor phase, and for a sinusoidal steady state s, we can write:

$$\overline{V_\mathrm{s}} = R_\mathrm{s}\overline{I_\mathrm{s}} + j\omega_\mathrm{s}(L_\mathrm{s}^s\overline{I_\mathrm{s}} + M^s\overline{I_\mathrm{r}})$$
$$\overline{0} = \frac{R_\mathrm{r}}{g}\overline{I_\mathrm{r}} + j\omega_\mathrm{s}(M^s\overline{I_\mathrm{s}} + L_\mathrm{r}^s\overline{I_\mathrm{r}})$$

where:

$$\overline{V_\mathrm{s}} = V_\mathrm{s}$$
$$\overline{I_\mathrm{s}} = I_\mathrm{s}\mathrm{e}^{-j\zeta_1}, \zeta_1 = \angle(\overline{V_\mathrm{s}}, \overline{I_\mathrm{s}})$$
$$\overline{I_\mathrm{r}} = I_\mathrm{r}\mathrm{e}^{-j\zeta_2}, \zeta_2 = \angle(\overline{V_\mathrm{s}}, \overline{I_\mathrm{r}})$$

g is the slip.

The equivalent circuit is shown in Figure 3.

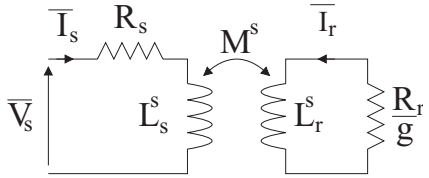

Fig. 3. Equivalent circuit of the induction machine for a certain saturation level.

To obtain the electrical parameters shown from the stator, we introduce the magnetizing stator current $\overline{I_\mathrm{ms}} = \overline{I_\mathrm{s}} + \frac{M^s}{L_\mathrm{s}^s}\overline{I_\mathrm{r}}$ and the rotor current shown from the stator $\overline{I'_\mathrm{r}} = \frac{M^s}{L_\mathrm{s}^s}\overline{I_\mathrm{r}}$ (Fig. 4):

$$\overline{V_\mathrm{s}} = R_\mathrm{s}\overline{I_\mathrm{s}} + j\omega_\mathrm{s}L_\mathrm{s}^s\overline{I_\mathrm{ms}}$$
$$\overline{0} = \frac{R'_\mathrm{r}}{g}\overline{I'_\mathrm{r}} + j\omega_\mathrm{s}(L_\mathrm{s}^s\overline{I_\mathrm{s}} + N^s\overline{I'_\mathrm{r}})$$

where $N^s = L_\mathrm{s}^s\left(\frac{L_\mathrm{s}^s L_\mathrm{r}^s}{(M^s)^2} - 1\right)$ is the leakage inductance totaled in the rotor, and $R'^s_\mathrm{r} = \left(\frac{L_\mathrm{s}^s}{M^s}\right)^2 R_\mathrm{r}$ is the rotor resistance shown from the stator which depends on the magnetic state of the machine.

We call the model presented in Figure 4 the steady state model with leakage inductance totaled in the rotor for a certain saturation level.

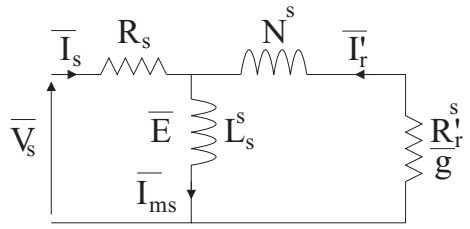

Fig. 4. Steady state model with leakage inductance totaled in the rotor.

4 New experimental measurement method of electrical parameters of the steady state model with leakage inductance totaled in the rotor for several saturation levels

Now, we will search a new experimental measurement method of the electrical parameters of the circuit shown in Figure 4 for several saturation levels s.

1- The stator resistance R_s does not depend on the magnetic state of the machine, so we can measure it by applying a continuous stator voltage on one of the stator phases.

2- To measure L_s we propose to do several no-load measurements for several amplitudes of the stator voltage and at a fixed frequency smaller than the nominal frequency. The circuit employed in this case is the following:

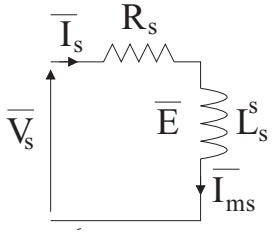

Fig. 5. No-load circuit of the induction machine.

For each magnitude of the stator voltage, the value of $L_\mathrm{s}^{s_i}$ corresponding to the steady state s_i is calculated using the following expression:

$$L_\mathrm{s}^{s_i}\left(\left|\underline{I_\mathrm{m}^{s_i}}\right|\right) = \frac{3(E_\mathrm{rms}^s)^2}{\omega_\mathrm{s}Q^{s_i}} \quad (8)$$

where Q is the reactive power.

3- To calculate rotor parameters shown from the stator for several saturation level, we propose to do several experimental measurements at a small slip and at a stator frequency smaller than the nominal one. The reason of these conditions is that the induction machine can not be saturated if we apply the classical measurement method when the rotor is blocked.

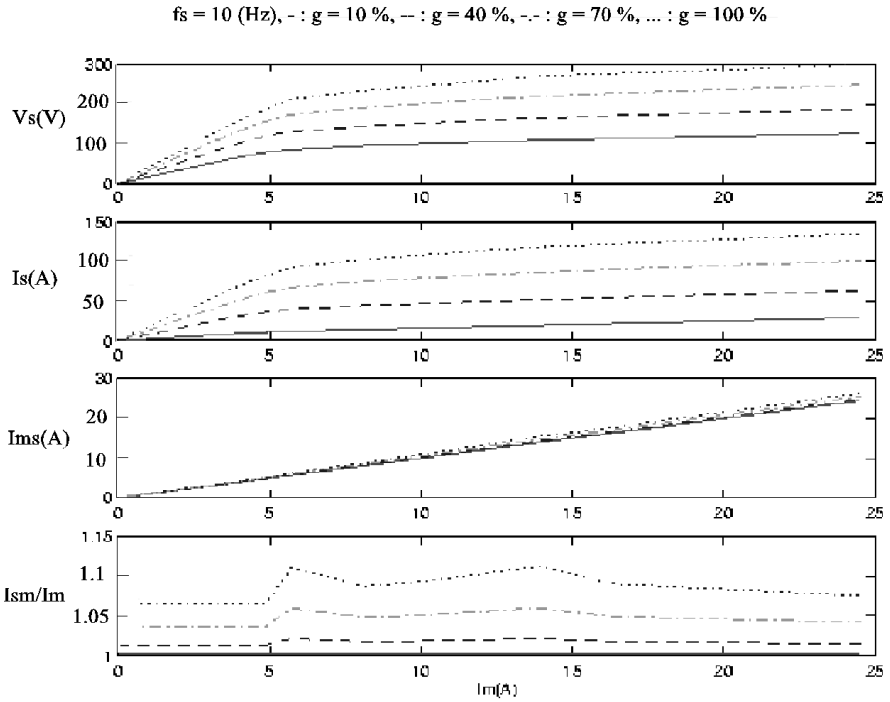
fs = 10 (Hz), - : g = 10 %, -- : g = 40 %, -.- : g = 70 %, ... : g = 100 %
Vs(V)
Is(A)
Ims(A)
Ism/Im
Im(A)

Fig. 6.

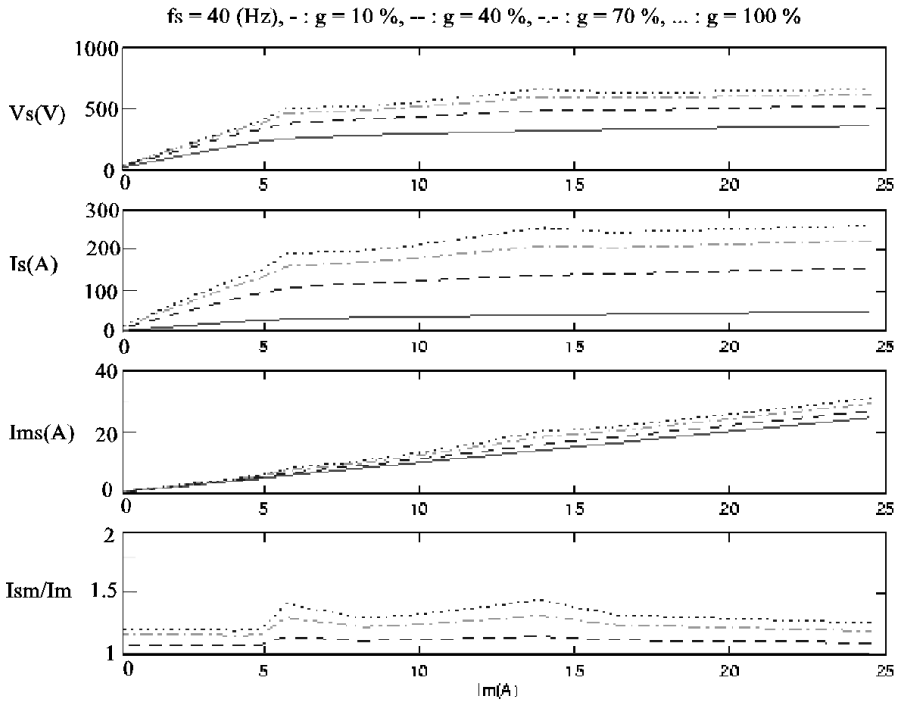
fs = 40 (Hz), - : g = 10 %, -- : g = 40 %, -.- : g = 70 %, ... : g = 100 %
Vs(V)
Is(A)
Ims(A)
Ism/Im
Im(A)

Fig. 7.

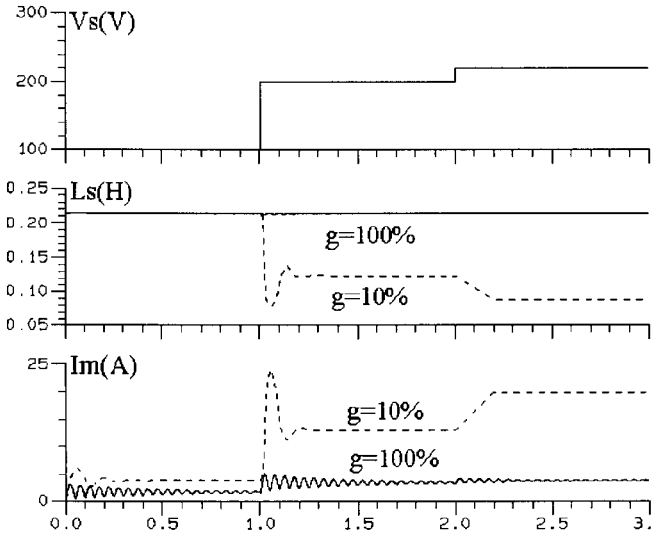

Fig. 8. Simulation example for a small slip and for a blocked rotor.

To demonstrate this idea, we develop the following study using the cyclic inductances curves obtained for a 4 KW induction machine and calculated by a finite elements calculation program [5,6]. From Figure 4 and for a steady state s_i we have:

$$\overline{V_{\rm s}^{s_i}} = R_{\rm s}\overline{I_{\rm s}^{s_i}} + Z_{L_{\rm s}}^{s_i}\overline{I_{\rm ms}^{s_i}} \tag{9}$$

$$\overline{I_{\rm ms}^{s_i}} = \left(1 + \left(\frac{L_{\rm s}^{s_i}}{M^{s_i}} - 1\right)\frac{Z_{L_{\rm s}}^{s_i}}{Z_{\rm rotor}^{s_i}}\right)^{-1}\overline{I_{\rm m}^{s_i}} \tag{10}$$

$$\overline{I_{\rm s}^{s_i}} = \left(1 - \frac{Z_{L_{\rm s}}^{s_i}}{Z_{\rm rotor}^{s_i}}\right)\left(1 + \left(\frac{L_{\rm s}^{s_i}}{M^{s_i}} - 1\right)\frac{Z_{L_{\rm s}}^{s_i}}{Z_{\rm rotor}^{s_i}}\right)^{-1}\overline{I_{\rm m}^{s_i}} \tag{11}$$

where $Z_{L_{\rm s}}$ is the impedance of $L_{\rm s}$ and $Z_{\rm rotor}$ is the impedance of the rotor circuit.

From these previous equations we obtain Figures 6 and 7.

We notice, from these figures, that it is very difficult to saturate the machine for high values of the slip and the stator frequency.

To illustrate the previous study, we show in Figure 8 two simulated dynamic responses of the 4 KW machine for a slip of 100% and for 10%. It is clear that the machine can be easily saturated if the value of the slip is small.

Therefore, to calculate $R'_{\rm r}$ and N for several saturation levels, we have to do measurements at a small value of the slip to obtain a weak value of the rotor current shown from the stator which opposes to the stator current, and at a stator frequency smaller than the nominal frequency to have a small impedance of the inductance $L_{\rm s}$.

For each steady state s_i, determined by the magnitude of the stator voltage $V_{\rm s}^{s_i}$, and for a fixed stator frequency, the values of $R'_{\rm r}$ and N are calculated from Figure 4 using the following expressions:

$$R_{\rm r}'^{s_i} = g^{s_i}P_1^{s_i}\frac{3(E_{\rm eff}^{s_i})^2}{(P_1^{s_i})^2 + (Q_1^{s_i})^2} \tag{12}$$

$$N^{s_i} = \frac{Q_1^{s_i}}{\omega_{\rm s}}\frac{3(E_{\rm eff}^{s_i})^2}{(P_1^{s_i})^2 + (Q_1^{s_i})^2} \tag{13}$$

$$P_1^{s_i} = P^{s_i} - 3(I_{\rm seff}^{s_i})^2 R_{\rm s} \tag{14}$$

$$Q_1^{s_i} = Q^{s_i} - \frac{3(E_{\rm eff}^{s_i})^2}{\omega_{\rm s}L_{\rm s}^{s_i}} \tag{15}$$

where P and Q are the active and the reactive powers.

From equation (15) we notice that we have to know the value of the stator cyclic inductance for each experiment. This value can be calculated by doing the approximation $\overline{I_{\rm ms}^{s_i}} \approx \overline{I_{\rm m}^{s_i}}$ (small slip) and by using the approximated equation:

$$E^{s_i} \approx \sqrt{\frac{2}{3}}\omega_{\rm s}L_{\rm s}^{s_i}\left|\underline{I_{\rm m}^{s_i}}\right|. \tag{16}$$

So, for each experiment we measure E^{s_i} and we search the intersection point between the curve $L_{\rm s}^{s_i}\left|\underline{I_{\rm m}^{s_i}}\right|$, found by doing the no load experiments, and $\sqrt{\frac{3}{2}}\frac{E^{s_i}}{\omega_{\rm s}}$.

5 Application of the new experimental measurement method on a 4 KW squirrel cage induction machine

We apply the new measurement method on a machine of 4 KW. This machine is loaded with a velocity controlled synchronous machine, Figure 9.

The stator frequency can be changed using a PWM inverter.

The measurements are done at a stator frequency of 20 Hz, and the measurements of the rotor parameters shown from the stator are done at a slip of 10%. The results obtained by the new experimental measurement method are presented in Figures 10 and 11.

The evolution obtained of the inductance $L_{\rm s}$ with these measurements is very close to the evolution calculated with a finite elements calculation program.

From Figure 11, and for the measurements at a small slip of rotor parameters shown from the stator, we notice that the values of the total leakage inductance N experimentally measured are bigger than those calculated using a finite elements calculation program. This can be explained by the fact that the finite elements calculation program is a two-dimension program and it does not take in to account all leakage inductances.

Here, we mention that this method has a weak sensitivity in measuring several points when the machine starts to be saturated, Figure 10. This is because of the big variation of the cyclic inductances for a small variation of the stator voltage. This is why we obtain an irregular curve in this zone.

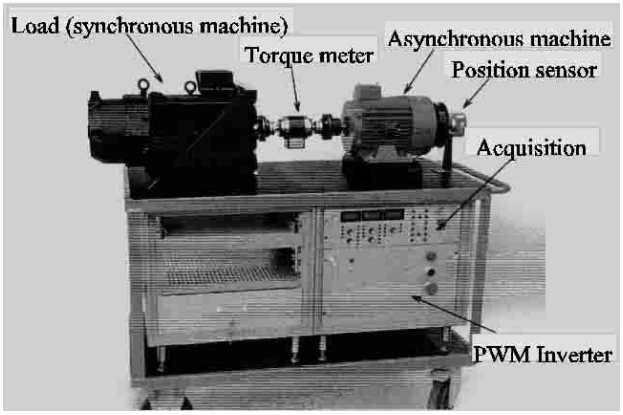

Fig. 9. Electromechanical system used to measure the electrical parameters shown from the stator.

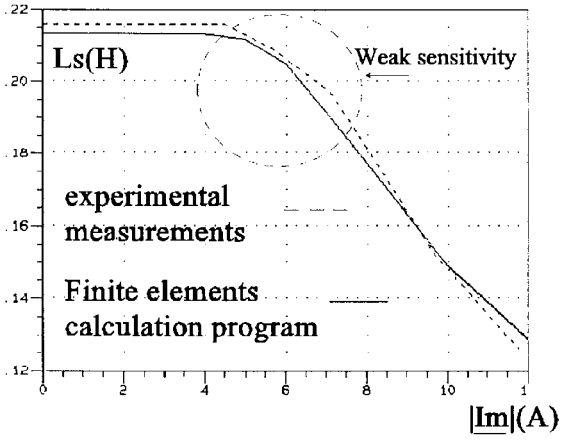

Fig. 10. Results of no load experiments.

6 Establishment of a new dynamic saturated model of the induction machine

Now, we will find another two-phase saturated model that only needs the electrical parameters shown from the stator.

From equation (6) we can write the stator flux vector as follows:

$$\underline{\Phi_{\rm s}} = L_{\rm s}\underline{I_{\rm ms}} \tag{17}$$

where $\underline{I_{\rm ms}} = \underline{I_{\rm s}} + \frac{M}{L_{\rm s}}\underline{I_{\rm r}} = \underline{I_{\rm s}} + \underline{I'_{\rm r}}$ is the magnetizing stator current vector.

We add and substrate $\frac{M^2}{L_{\rm s}}\underline{I_{\rm r}}$ from the expression of the rotor flux vector, then we multiply it by $\frac{L_{\rm s}}{M}$:

$$\underline{\Phi'_{\rm r}} = (L_{\rm s} + N)\underline{I'_{\rm r}} + L_{\rm s}\underline{I_{\rm s}} \tag{18}$$

where $\underline{\Phi'_{\rm r}} = \frac{L_{\rm s}}{M}\underline{\Phi_{\rm r}}$ and $N = L_{\rm s}\left(\frac{L_{\rm s}L_{\rm r}}{M^2} - 1\right)$ is the leakage inductance totaled in the rotor.

If we introduce the new vectors $\underline{\Phi'_{\rm r}}$ and $\underline{I'_{\rm r}}$ in the electrical equations (5), we obtain a new two-phase saturated model that can be described by:

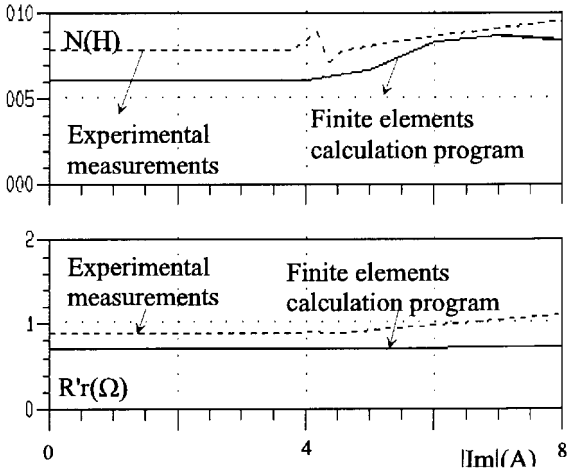

Fig. 11. Results of small slip experiments.

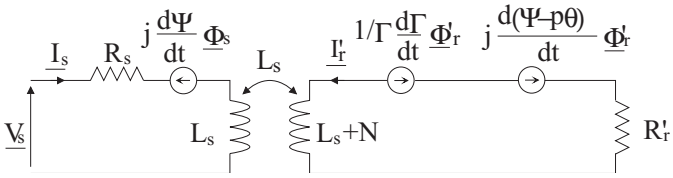

Fig. 12. Two-phase saturated model with leakage inductance totaled in the rotor.

– electrical equations:

$$\begin{aligned}\underline{V_{\rm s}} &= R_{\rm s}\underline{I_{\rm s}} + \frac{{\rm d}\underline{\Phi_{\rm s}}}{{\rm d}t} + j\frac{{\rm d}\Psi}{{\rm d}t}\underline{\Phi_{\rm s}} \\ \underline{0} &= R'_{\rm r}\underline{I'_{\rm r}} + \frac{{\rm d}\underline{\Phi'_{\rm r}}}{{\rm d}t} + \frac{1}{\Gamma}\frac{{\rm d}\Gamma}{{\rm d}t}\underline{\Phi'_{\rm r}} + j\frac{{\rm d}(\Psi - p\theta)}{{\rm d}t}\underline{\Phi'_{\rm r}}\end{aligned} \tag{19}$$

where $\Gamma = \frac{M}{L_{\rm s}}$

– flux-current relationships:

$$\begin{aligned}\underline{\Phi_{\rm s}} &= L_{\rm s}\underline{I_{\rm ms}} \\ \underline{\Phi'_{\rm r}} &= (L_{\rm s} + N)\underline{I'_{\rm r}} + L_{\rm s}\underline{I_{\rm s}}\end{aligned} \tag{20}$$

– mechanical equation:

$$j\frac{{\rm d}\Omega}{{\rm d}t} = C_{\rm em} - f\Omega - C_{\rm r}. \tag{21}$$

The electrical circuit of this model is shown in Figure 12.

To resolve the electromechanical equations of this new model, we have to do the approximation $\Gamma \approx \frac{L_{\rm s}}{L_{\rm s}+N}$ and apply the same algorithm used to solve the electromechanical equations of the two-phase saturated model of separated leakage inductances which we presented in paper [5].

7 Experimental validation

Figure 13 shows the real dynamic responses of the 4 KW machine (curves 1) with the dynamic responses of the

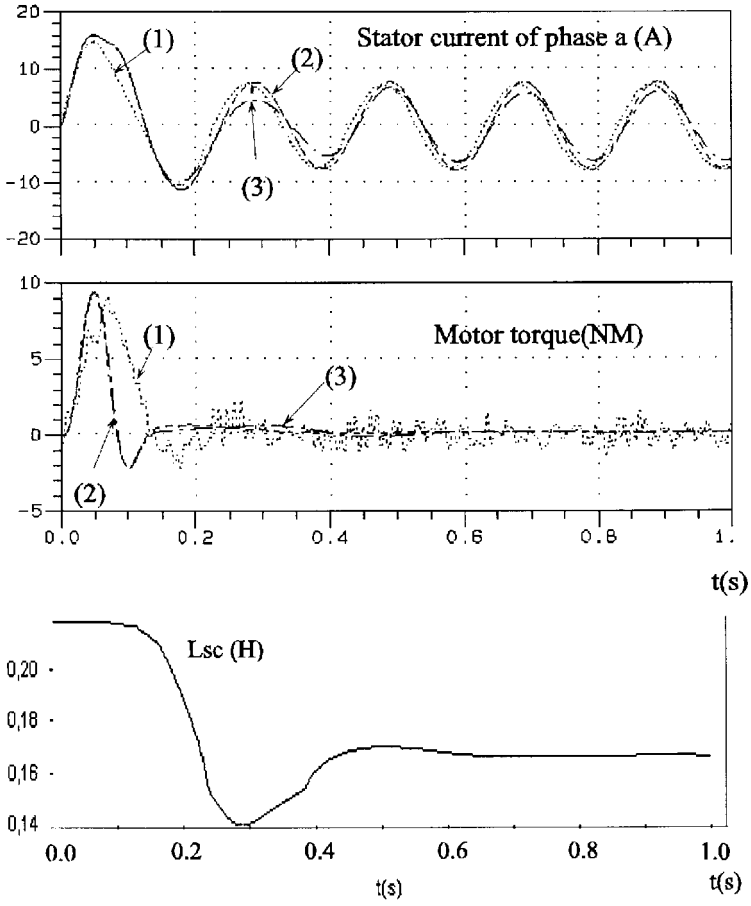

Fig. 13. Dynamic responses of the 4 KW machine. (1) Real response. (2) Saturated model. (3) Linear model.

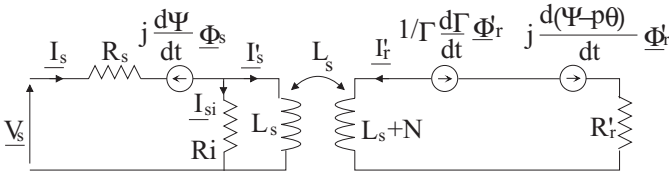

Fig. 14.

same machine modeled by the linear two phase model at nominal values of cyclic inductances (curves 3) and by the two-phase saturated model with leakage inductance totaled in the rotor (curves 2). We can clearly see that the last model gives closer dynamic responses to the real dynamic responses of the machine.

The experiments are done at a maximum magnitude of the stator voltages of $V_s = 40$ V, and at a stator voltages frequency of $f_s = 5$ Hz. So, under these conditions, we are sure that the machine has a greater saturation level than the nominal saturation level which is given at $V_s = 311$ V and at $f_s = 50$ Hz. We can also see from the previous figure that the stator cyclic inductance is 23.8% smaller than its linear value.

8 Remarks

In this paper we do not take into account the iron losses. This can be introduced by adding a resistance R_i in parallel with L_s. We can measure this resistance while doing the second step of the new experimental measurement method using the expression:

$$R_i = \frac{3E_{\text{eff}}^2}{p - 3R_s I_{\text{seff}}^2}$$

in this case, the electrical equations (19) stay the same, but the cyclic inductances vary with $\left|\underline{I_m}\right| = \left|\underline{I'_s}\right| + \left|\underline{I'_r}\right|$ where $\underline{I'_s} = \underline{I_s} - \underline{I_{si}}$ and $\underline{I_{si}}$ is the current of the resistance R_i, Figure 14.

9 Conclusion

In this paper we presented a new experimental measurement method of the electrical parameters of the induction machine shown from the stator. This method was applied on a 4 KW induction machine and validated by comparing its results with the results obtained by a finite elements calculation program. The aim of searching such a method is to find a new two-phase saturated model that uses the electrical parameters measured from the stator.

This model was called the two-phase saturated model with leakage inductance totaled in the rotor.

The study has a very big advantage from the industrial point of view, especially for a squirrel cage induction machine. It avoids the use of a finite elements calculation program to calculate the evolution of cyclic inductances with the variation of saturation level in the air gap. By doing the proposed experiments, which are relatively simple, we can find the evolutions of the electrical parameters of the machine shown from the stator and then use the new two-phase saturated model with leakage inductance totaled in the rotor.

References

1. J.C. Chalmers, R. Dodgson, IEEE Trans. Power Appar. and Syst. **90**, 564 (1971).
2. O. Ojo, M. Vipin, I. Bhat, IEEE Trans. Ind. Appl. **30**, 1638 (1994).
3. P. Vas, M. Alakula, IEEE Trans. Energy Conversion **5**, 218 (1990).
4. R.D. Lorenz, D.W. Novotny, IEEE Trans. Ind. Appl. **26**, 283 (1990).
5. T. Kasmieh, Y. Lefevre, X. Roboam, J. Faucher, Eur. Phys. J. AP **1**, 57 (1998).
6. T. Kasmieh, Modélisation et caractérisation de la saturation magnétique des machines asynchrones en vue de la commande, thèse de doctorat, LEEI-INPT, Toulouse, France, 1998.
7. B. Semail, Modélisation et réalisation d'un actionneur asynchrone et de sa commande vectorielle, thèse de doctorat, LGEP, Paris IV, France, 1990.
8. D. Bajodeck, Modèle multi-enroulement de la machine asynchrone, stage de DEA, LEEI-INPT, Toulouse, France, 1994.
9. N. Sadowski, Modélisation des machines électriques à partir de la résolution des équations du champs en tenant compte du mouvement et du circuit d'alimentation (logiciel EFCAD), thèse de doctorat, LEEI-INPT, Toulouse, France, Octobre 1997.
10. B. Lemaire-Semail, J.P. Louis, F. Bouillaut, Eur. Phys. J. AP **5**, 257 (1998).